Microbiology (2005), **151**, 1569–1576 DOI 10.1099/mic.0.27536-0

Phenotypic differentiation and seeding dispersal in non-mucoid and mucoid *Pseudomonas aeruginosa* biofilms

B. Purevdorj-Gage,[1] W. J. Costerton[1] and P. Stoodley[1,2]

[1]Center for Biofilm Engineering, 366 EPS Building – PO Box 173980, Montana State University-Bozeman, MT 59717, USA

[2]Center for Genomic Sciences, Allegheny-Singer Research Institute, Pittsburgh, USA

Correspondence
B. Purevdorj-Gage
laura_p@erc.montana.edu

Received 2 August 2004
Revised 9 December 2004
Accepted 3 February 2005

There is growing evidence that *Pseudomonas aeruginosa* biofilms exhibit a multicellular developmental life cycle analogous to that of the myxobacteria. In non-mucoid PAO1 biofilms cultured in glass flow cells the phenotypic differentiation of microcolonies into a motile phenotype in the interior of the microcolony and a non-motile surrounding 'wall phenotype' are described. After differentiation the interior cells coordinately evacuated the microcolony from local break out points and spread over the wall of the flow cell, suggesting that the specialized microcolonies were analogous to crude fruiting bodies. A microcolony diameter of approximately 80 μm was required for differentiation, suggesting that regulation was related to cell density and mass transfer conditions. This phenomenon was termed 'seeding dispersal' to differentiate it from 'erosion' which is the passive removal of single cells by fluid shear. Using the flow cell culturing method, in which reproducible seeding phenotype in PAO1 wild-type was demonstrated, the effects of quorum sensing (QS) and rhamnolipid production (factors previously identified as important in determining biofilm structure) on seeding dispersal using knockout mutants isogenic with PAO1 was investigated. Rhamnolipid (*rhlA*) was not required for seeding dispersal but *las*/*rhl* QS (PAO1-JP2) was, in our system. To assess the clinical relevance of these data, mucoid *P. aeruginosa* cystic fibrosis isolate FRD1 was also investigated and was seeding-dispersal-negative.

INTRODUCTION

The proliferation and persistence of bacterial biofilms on various surfaces have been well documented in both *in vitro* and *in vivo* settings, and modern microscopic as well as molecular techniques have revealed that biofilm formation is a complex multifactorial process regulated by both genetic and environmental factors (Stoodley *et al.*, 2002). Although much is known about the initial stages of biofilm development, very little is known about the mechanisms governing the detachment process (Stewart 1993; Stewart *et al.*, 2000). Detachment has been shown to play an important role in shaping the morphological characteristics and structure of mature biofilms (Picioreanu *et al.*, 2001; Stewart 1993; Van Loosdrecht *et al.*, 1995, 1997) which further extends the implication of this process in biofilm function and behaviour in general. Other studies have characterized two main types of detachment processes: erosion (the continual detachment of single cells and small portions of the biofilm) and sloughing (the rapid, massive loss of biofilm) (Bryers, 1988; Characklis, 1990; Stoodley *et al.*, 2001). However, these types of detachment were generally thought of in terms of passive, shear-dependent processes. Only recently has detachment been considered as an active dispersal mechanism. A number of laboratories have observed the 'hollowing' out of microcolonies by cells actively leaving the interiors (Sauer *et al.*, 2002) and the remaining 'hollow mounds' have been noted in *Pseudomonas putida* biofilms (Tolker-Nielsen *et al.*, 2000). Based on previous reports, the suggested mechanisms for this particular hollowing process in the biofilm clusters differ from one biofilm species to another. For example, Kaplan *et al.* (2003b) have shown that the 'non-motile' Gram-negative bacterium *Actinobacillus actinomycetemcomitans*, grown statically on agar, released individual cells from within the biofilm colony via enzymic activity of β-hexosaminidase (Kaplan *et al.*, 2003a). On the other hand transmission electron micrographs of *Staphylococcus epidermidis* cultured on agar plates suggested that the hollowing process may have occurred through the process of cell lysis (P. Stewart, personal communication). Also, Webb *et al.* (2003) have demonstrated that the cells in the interior of *P. aeruginosa* clusters lysed via phage

Abbreviations: CF, cystic fibrosis; QS, quorum sensing.

The online version of this paper at http://mic.sgmjournals.org has supplementary movie files.

infection, which resulted in the formation of a structurally differentiated biofilm cluster.

In previous experiments (Purevdorj-Gage & Stoodley, 2004) we reported hollow areas inside clusters of non-mucoid *P. aeruginosa* PAO1 grown in flow cells on Luria–Bertani (LB) medium. We hypothesized that these hollow mounds were linked to an active dispersal process. It was the goal of this work to quantify the progression and dimensions of biofilm colonies as well as to document the dispersion of cells from the microcolonies in the flowing system. Biofilms of non-mucoid *P. aeruginosa* PAO1 wild-type, isogenic rhamnolipid-deficient strain PAO1-Δ*rhlA*, PAO1-Δ*lasI*Δ*rhlI* null mutant JP2 strain and cystic fibrosis (CF) clinical isolate *P. aeruginosa* FRD1 were grown in a once-through flow system. A digital time lapse imaging microscope and a scanning laser confocal microscope were used for visualization and quantification. The effects of rhamnolipid and quorum sensing (QS) deficiency on seeding dispersal were of particular interest, since these factors are actively involved in *P. aeruginosa* biofilm structural development (Davies *et al.*, 1998) as well as in maintaining the void channels within the biofilms (Davey *et al.*, 2003).

Since cells in the periphery of microcolonies became highly agitated as a prelude to seeding dispersal, we also investigated various aspects of motility by performing swimming, swarming and twitching assays on LB agar using each of the four strains. To determine the potential of biofilm viscosity to affect motility of single cells within the biofilm matrix, we measured the viscoelasticity of PAO1 and FRD1 microcolonies using rheometry.

METHODS

Bacterial strains and medium. Biofilms were grown from the *P. aeruginosa* strains listed in Table 1. LB full-strength broth (20 g l^{-1}) was used as the growth medium for biofilms and 24 h shake flask cultures were used for initial inoculation with an appropriate selective antibiotic.

Biofilm culture flow cell system. Biofilms were grown in 1 mm × 1 mm square glass capillary (Friedrick & Dimmock) flow cells, which were incorporated into a once-through flowing system (Stoodley *et al.*, 1999). A sterile nutrient medium was pumped through the system via a peristaltic pump at flow rate of 1·0 ml min^{-1}. At this flow rate flow was laminar with a Reynolds number of 16 and a shear stress of 0·3 Pa along the centre of the lumen. The flow cells were positioned in a polycarbonate holder which was mounted on the stage of an Olympus BH2 upright microscope so that the biofilm could be imaged *in situ* without interrupting flow. A septum-sealed inoculation port was positioned upstream of the flow cell, through which the initial load of bacterial cells were introduced to the system. Triplicate flow cell experiments were run for 5 days for *P. aeruginosa* PAO1, FRD1 and duplicate experiments for PAO1(pMF230), PAO1-Δ*rhlA* and PAO1-Δ*lasI*Δ*rhlI* mutants with two replicate flow cells for each experiment resulting in four individual biofilms for each mutant type. Under operating conditions the water temperature in the reactor system was 23 °C and all experiments were performed at this temperature.

Reactor sterilization. The reactor system was autoclaved at 121 °C for 15 min. The sterility of the reactor system was confirmed by plating 0·1 ml aliquots of effluent onto LB agar (LA). Pure culture and conversion of mucoidy (for *P. aeruginosa* FRD1) flow cell experiments were confirmed through visual examination of colonies grown by plating 0·1 ml aliquots of effluent onto solid LA on a daily basis. Effluent from the PAO1-Δ*rhlA* and PAO1-Δ*lasI*Δ*rhlI* biofilms was plated onto LA plates and LA plates with appropriate selective antibiotics to confirm integrity of the mutations. There was no statistical difference between the c.f.u. counted between LA and LA plates with selective markers (all P values > 0·05).

Inoculum and medium. The reactor containing full-strength LB was inoculated with 1 ml of an overnight full-strength LB 37 °C shake flask culture of micro-organisms. The flow system was allowed to sit for 30 min, to permit attachment, before switching to continuous culture. The system was then switched to continuous culture mode by delivering LB to the mixing chamber via a peristaltic pump (Cole Parmer #7553-80). Effluent samples were taken periodically to monitor the detached population and to confirm culture purity.

Microscopy. The developing biofilm was visualized *in situ* by using transmitted light and ×5, ×10 and ×50 objective lenses with an Olympus BH2 microscope. Images were collected using a COHU 4612-5000 CCD camera and captured with a Scion VG-5 PCI framestone board. Scion Image software was used to collect time-lapse sequences and for image enhancement and analysis. A 1 mm graticule with 10 μm divisions was used to calibrate length measurements. The biofilm thickness and surface area coverage were measured on each day at five random locations in the biofilm area for each flow cell experiment (Stoodley *et al.*, 1999). The diameters of individual microcolonies were also measured using Scion Image. We estimated that for the particular settings of the light microscope, we could confidently resolve individual cell clusters down to diameters of approximately 10 μm.

Rheometry experiments. To investigate the role of biofilm viscosity on seeding dispersal, PAO1 and FRD1 biofilms were grown on LA plates for 48 h at 36 °C. The colonies were aseptically scraped off the agar surface and used for rheometry measurements according to Towler *et al.* (2003). Two individual agar plates were used for each individual measurement. A total of eight replicate measurements

Table 1. A list of strains, sources and descriptions

Strain (reference)	Genotype	Phenotype and description
PAO1 (Pearson *et al.*, 1997)	*P. aeruginosa* PAO1	Wild-type
PAO1-Δ*lasI*Δ*rhlI* (JP2) (Pearson *et al.*, 1997)	*P. aeruginosa* PAO1 Δ*lasI*::Tn*10* Tc^r; Δ*rhlI*::Tn*501* Hg^r	QS-negative
PAO1-Δ*rhlA* (Ochsner *et al.*, 1994)	*P. aeruginosa* Δ*rhlA*::Gm^r	Rhamnolipid-negative
PAO1-Δ*fliM* (Klausen *et al.*, 2003)	*P. aeruginosa* Δ*fliM*::Tn*5B30* Tc^r	Flagella-negative
PAO1 (Nivens *et al.*, 2001)	*P. aeruginosa* PAO1(pMF230) *mut2* Ca^r	Constitutive GFP
FRD1 (Ohman & Chakrabarty, 1981)	CF patient isolate, *mucA22* Alg^+	Mucoid

from PAO1 and seven from FRD1 were performed for statistical comparisons. The viscosity was measured from creep tests using a TA Instruments AR 1000 Rheometer (info@tainst.com) in which the resultant strain in response to an applied shear stress of 0·5 or 1 Pa was measured over time.

Motility assay. Sterile LA plates with varying concentrations of agarose [0·3 % for swimming (Kohler *et al.*, 2000), 1·3 % for swarming (Aendekerk *et al.*, 2002), 1·0 % for twitching assay (Semmler *et al.*, 1999), 1·5, 3 and 5 % for rheometry experiments] were prepared. Equal concentrations of bacterial cultures (OD_{600}) were stab-inoculated into the agar plates with a sterile toothpick. The plates were inverted and incubated at 36 °C for 16 h. The diameter of the zone of spreading from the inoculation point was then measured. Twelve replicate measurements were performed for each strain tested.

RESULTS

Flow cell PAO1 and FRD1 biofilms

Twenty-four hours post-inoculation (day 1) both PAO1 and FRD1 biofilms consisted of a sparse single layer of cells. By the second day PAO1 had formed 20 ± 4 μm (mean $\pm$ SD, $n=5$) thick biofilms with hemispherical microcolonies 70 ± 30 μm ($n=30$ individual clusters) in diameter. The FRD1 biofilm was 16 ± 3 μm thick with similarly shaped clusters 30 ± 7 μm ($n=30$ individual clusters) in diameter. Between the colonies there was a monolayer of cells so that the surface area coverage at this time had reached 100 % in the two biofilms. Throughout the remainder of the experimental run time the thickness and surface area cover did not change in the PAO1 biofilm (P values $>0{\cdot}05$), so that by day 5 it was 20 ± 2 μm thick and covered the entire surface of the glass flow cell (Fig. 1a). There were no significant differences between the PAO1 and FRD1 daily thickness (all P values $>0{\cdot}05$) and surface area measurements (all P values $>0{\cdot}05$) on any of the 5 days. Similarly, by day 5 the mean cluster diameter in the FRD1 biofilm had reached 120 ± 50 μm, which was similar that measured in PAO1 (P values $>0{\cdot}05$). The visual organization of the cell clusters was also similar in the PAO1 and FRD1 biofilms up to day 2. However, by day 3 we observed a prominent difference in the appearance of the mature clusters formed by the two

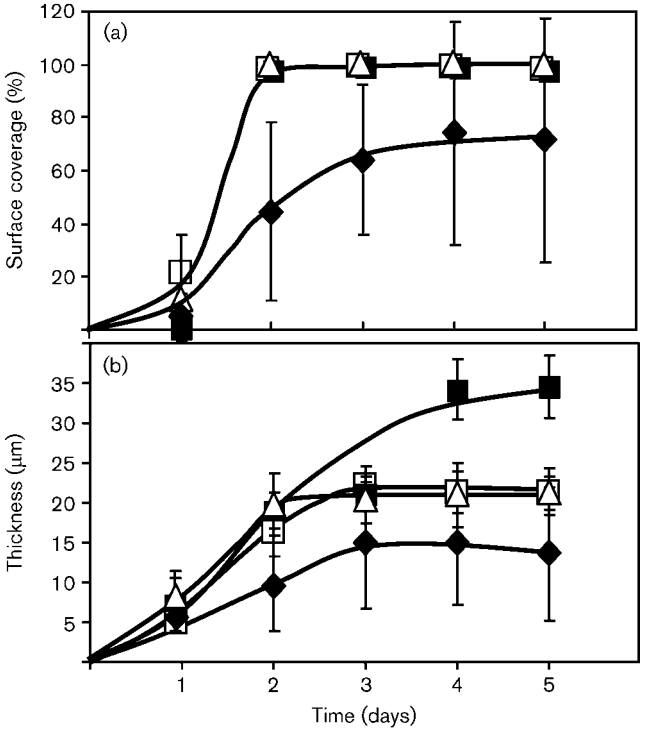

Fig. 1. Temporal development of various biofilms quantified by surface coverage (a) and thickness (b). PAO1 (open triangles), FRD1 (open squares), Δ*rhlA* mutant (filled squares) and PAO1-Δ*lasI*Δ*rhlI* (filled diamonds) biofilms. Error bars indicate 1 SD ($n=15$) from at least four individual biofilms.

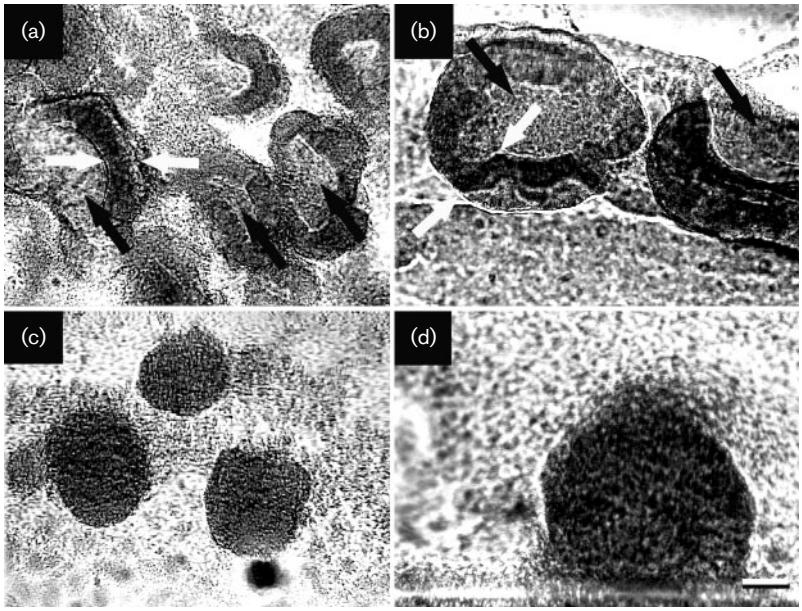

Fig. 2. PAO1 (a), Δ*rhlA* mutant (b), FRD1 (c) and PAO1-Δ*lasI*Δ*rhlI* (d) biofilms cultivated in the flow cell system. Hollow mounds were evident in 5-day-old mature PAO1 biofilm clusters and 2-day-old Δ*rhlA* mutant biofilms. White arrows indicate the distinct 'walls' formed by non-motile cells and black arrows indicate void areas within individual microcolonies (a, b). FRD1 and PAO1-Δ*lasI*Δ*rhlI* biofilm clusters did not display the same structural characteristics and over the course of the experiment the microcolonies (dark clusters) did not hollow out. Bar, 20 μm; flow direction was from left to right.

biofilm types (Fig. 2). The larger PAO1 biofilm clusters had developed a hollow interior surrounded by a distinct shell-like wall of non-motile cells in all three replicate experiments, but the FRD1 clusters were consistently homogeneous and showed no evidence of hollowing. On closer inspection of the PAO1 biofilm, we observed that on day 3 the clusters had differentiated into two distinct cell phenotypes; highly motile cells in the interior of the clusters and cells which remained stationary making an outer cluster wall (Fig. 3). A movie documenting this phenomenon has been submitted as supplementary data ('Movie 1' available at http://mic.sgmjournals.org).

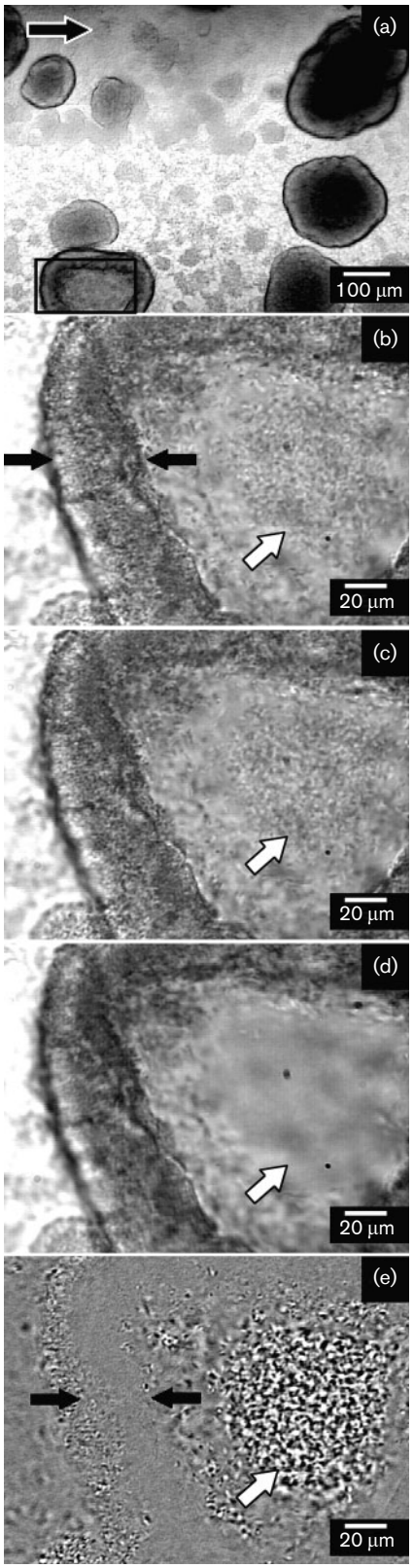

In some cases we observed the process of evacuation of cells out of clusters from local 'breakout' points in the walls which were at random locations and independent of the flow direction (Fig. 4). A movie showing cells evacuating a PAO1 microcolony has been submitted as supplementary data ('Movie 2' available at http://mic.sgmjournals.org). With continuous monitoring of the clusters from which the cells had evacuated, we noted that the remaining cluster walls did not exhibit further expansion and the central region of the cluster did not refill with new cell growth, but remained as a hollow mound (Fig. 5).

Quantification of developmental progression of cell clusters exhibiting seeding dispersal in PAO1

During the first 2 days of biofilm growth, $95 \pm 0{\cdot}05$ % ($n=3$ independent experiments) of all the clusters present in PAO1 biofilms appeared homogeneous without any obvious void areas; however, by day 3 as many as 46 ± 20 % clusters had developed hollow mounds at the central regions of the biofilm cluster and this increased up to 70 ± 20 % by day 5 (Fig. 6a). With closer analysis of these mounds, we determined that the void areas within the biofilm clusters gradually increased over time, but the thickness of the outer walls stayed roughly the same (Fig. 6c). Interestingly, the cluster measurement data show that there was a significant difference between the mean diameters of the hollow and non-hollow clusters ($P<0{\cdot}05$), indicating that clusters which were hollow were at least 80 μm thick (Fig. 6c).

Fig. 3. Time-lapse sequence demonstrating motile cells within 3-day-old biofilm microcolonies. (a) Low power magnification of biofilm clusters showing larger differentiated microcolonies (darker) interspersed with smaller, undifferentiated microcolonies (lighter). Panels (b–e) show higher power magnification of the cluster area indicated by the black rectangle in (a). Frames taken 1 s apart appeared similar (b and c, respectively), but by averaging 30 frames captured over a 1 s period the highly motile cells 'average' out and appear blurred in the centre of the microcolony (d), demonstrating the extent of the motile region (white arrow in panels b, c and d). The 'wall' region is indicated by the black arrows in (b) and (e). The motile interior was also demonstrated in (e) by subtracting (c) from (d) so that stationary regions, such as the 'wall' subtract out while the motile interior appears mottled.

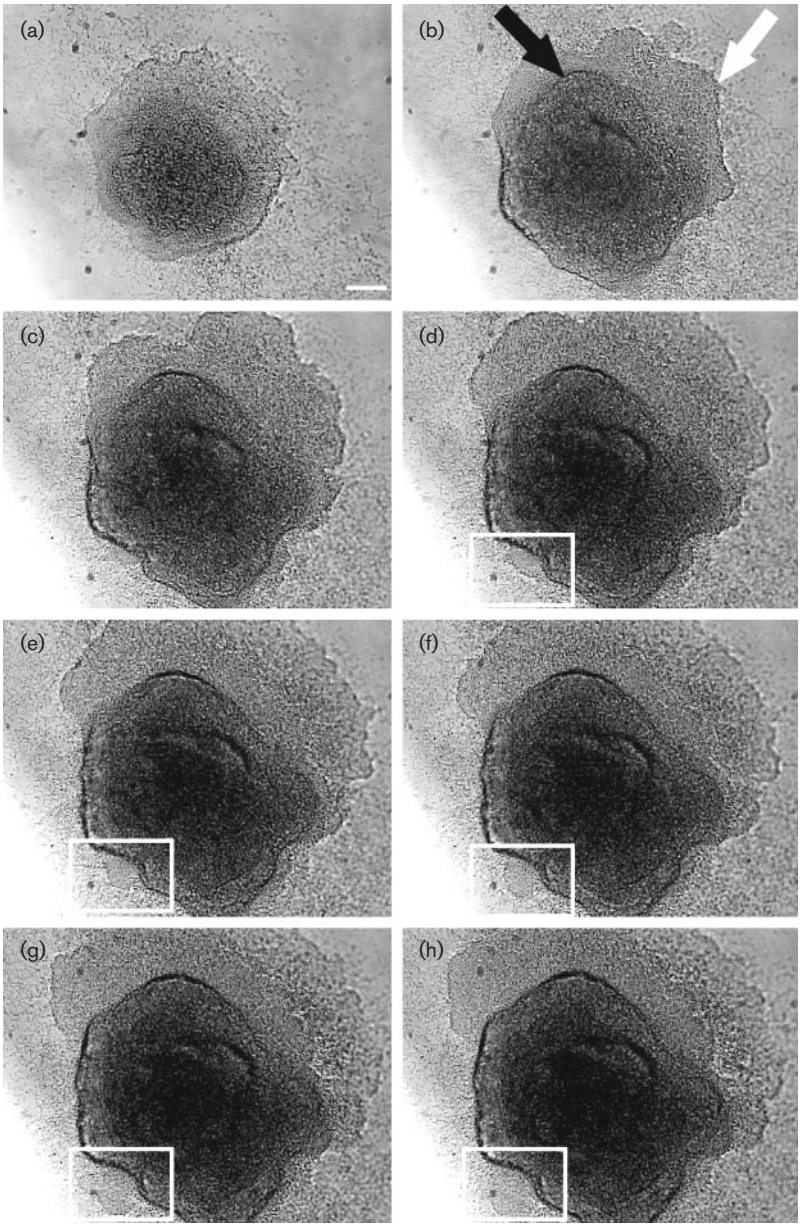

Fig. 4. Time-lapse sequence depicting seeding dispersal in a 3-day-old PAO1 biofilm cluster. The time interval between images was 15 min with the exception of 3 h between frames (a) and (b). The black arrow shows the immobile cluster wall whereas the white arrow indicates the dispersing cells. Another site of an evacuation 'bleb' is outlined by the white rectangle. Bar, 20 μm.

Involvement of rhamnolipid biosurfactant in the seeding dispersal

By day 2 the PAO1-Δ*rhlA* biofilm covered the entire surface of the flow cell, but during the last 2 days of the experimental run, its thickness reached 35 ± 5 μm (Fig. 1), which was significantly greater than that measured in both the PAO1 and FRD1 biofilms ($P < 0{\cdot}05$). Seeding dispersal and the resulting hollow biofilm mounds (Fig. 2b) with structural dimensions similar to PAO1 ($P = 0{\cdot}7$) were also evident in the Δ*rhlA* biofilm which also had a critical threshold diameter of approximately 80 μm (data not shown). While the hollow mounds in PAO1 biofilms persisted until the end of the experimental run time, the hollow mounds in PAO1-Δ*rhlA* had flattened into a homogeneous monolayer by days 4–5 (Fig. 6a).

Involvement of the QS system

In comparison to a wild-type biofilm, PAO1-Δ*lasI*Δ*rhlI* cells covered only about 40 % of the surface during the first 2 days ($P < 0{\cdot}05$). However, by day 4 the surface coverage was statistically similar to that measured in the PAO1 biofilm ($P > 0{\cdot}05$). Throughout the experimental run time there were no differences between wild-type and PAO1-Δ*lasI*Δ*rhlI* biofilm thicknesses ($P > 0{\cdot}05$). On day 3 a total of 97 clusters with a median diameter of 250 ± 150 μm were observed, of which none developed hollow structures during the full 5 days of growth (Fig. 2d). By the end of the experiment the biofilm covered the entire surface and thickness measurements were comparable to the wild-type biofilm (Fig. 1).

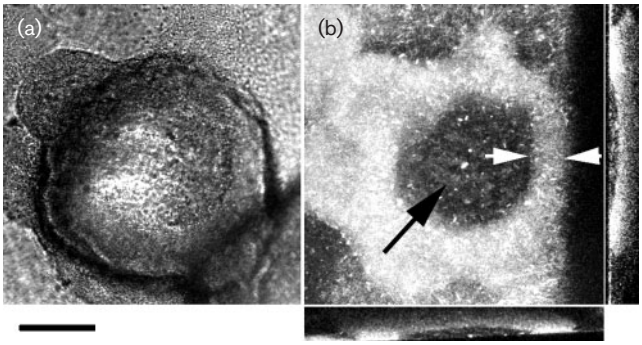

Fig. 5. A hollow mound formed by *P. aeruginosa* PAO1(pMF230) expressing GFP (day 5) shown using transmitted light (a) and a confocal slice through the biofilm cluster visualized through GFP expression (b). The black arrow indicates the hollow mound and two small white arrows indicate the walls of the cluster. The side panels are saggital *XZ* and *YZ* cross-sections through the microcolony showing the hollow interior (dark region). Bar, 40 μm.

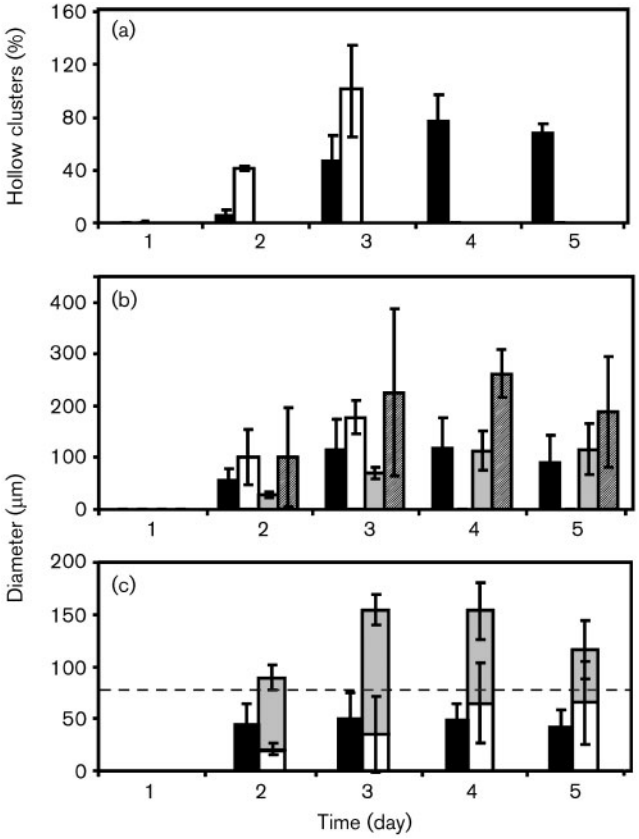

Fig. 6. Development of microcolonies in the *P. aeruginosa* biofilms. (a) Percentage of hollowed clusters in PAO1 (black bars), Δ*rhlA* (open bars), FRD1 (grey bars) and PAO1-Δ*lasI*Δ*rhlI* (hatched bars) biofilms over time (mean ± 1 SD from six independent biofilms from PAO1 and four from the Δ*rhlA* mutant). (b) Diameter (μm) of all cell clusters in PAO1 (black bars), PAO1-Δ*rhlA* mutant (open bars), FRD1 (grey bars) and PAO1-Δ*lasI*Δ*rhlI* (hatched bars) biofilms. (c) Temporal and structural development of hollow mounds in PAO1 clusters, quantified by the diameter of the non-hollow (black bars) and hollow (stacked bar) clusters. The stacked bars showing the dimensions of the hollow clusters also show the diameter of the empty area within the cluster (white portion) and the thickness of the wall × 2 (grey portion). Each point on the graph is a mean ± 1 SD from between 20 and 30 clusters from at least five individual images. A 'threshold diameter' of approximately 80 μm appears to be required for seeding dispersal from the interior of the clusters (indicated by a dashed line in panel c).

Motility assay in *P. aeruginosa* FRD1, PAO1 wild-type and its isogenic mutants

In addition to twitching (Semmler *et al.*, 1999) and swimming (Kohler *et al.*, 2000), swarming in *P. aeruginosa* has recently been discovered as a novel mode of coordinated propagation on a semisolid medium (Kohler *et al.*, 2000) and Aendekerk *et al.* (2002) have utilized LB medium solidified with 1·3 % agarose to test the swarming ability of various isogenic mutants in comparison to the PAO1 wild-type strain. Since coordinately moving cells were observed during the process of seeding dispersal, we investigated the ability of *P. aeruginosa* PAO1 isogenic Δ*rhlA* and Δ*lasI*Δ*rhlI* mutants, as well as mucoid strain FRD1, for twitching, swimming and swarming motility on LB agar, which to our knowledge has not been reported previously (medium composition is known to greatly affect the motility of *P. aeruginosa*; Rashid & Kornberg, 2000). All strains except FRD1 were able to form twitching, swimming and swarming colonies similar to previous descriptions (Semmler *et al.*, 1999; Aendekerk *et al.*, 2002) (data not shown).

Material properties of PAO1 and FRD1 biofilms

On 0·3 % agar (viscosity $3{\cdot}1 \times 10^5$ Pa s^{-1}) the swimming motility zone measured in PAO1-Δ*fliM* (Klausen *et al.*, 2003) and FRD1 strains was significantly less than that of PAO1 and PAO1-Δ*rhlA* (all P values $> 0{\cdot}05$; data not shown) and none of the strains was able to spread over the plate surface with an agar concentration of $\geqslant 1{\cdot}5$ % (viscosity $1{\cdot}4 \times 10^6$ Pa s^{-1}). Since agar viscosity has an important role in motility of our test strains, we wished to determine if the 'increased' viscosity associated with FRD1 may partly explain its deficiency in swimming motility. We performed creep curve tests to determine the difference in biofilm viscosity between mucoid and non-mucoid *P. aeruginosa* by culturing FRD1 and PAO1 biofilms on the surface of agar plates. Contrary to our expectations, we found that the FRD1 colonies were significantly less viscous ($4{\cdot}8 \times 10^5 \pm 0{\cdot}02 \times 10^5$ Pa s^{-1}, $n = 7$) compared to the PAO1 colonies ($5{\cdot}7 \times 10^5 \pm 0{\cdot}2 \times 10^5$ Pa s^{-1}, $n = 8$) ($P = 0{\cdot}014$).

DISCUSSION

Phenotypic differentiation in the 'seeding dispersal' behaviour

In this work we have documented a phenotypic differentiation of *P. aeruginosa* PAO1 biofilm microcolonies in a laboratory-based once-through flow system. This observation suggests that this organism exhibits functional co-ordinated multicellular behaviour associated with biofilm dispersal through the formation of specialized 'fruiting body'-like microcolonies. The release of single cells from PAO1 biofilms is consistent with the size distribution of detached biomass in which over 70 % of detachment events occurred as single cells (Wilson *et al.*, 2004). We suggest terming this active detachment process 'seeding dispersal' to differentiate it from 'erosion' which is associated with passive, shear-mediated detachment. Microcolony differentiation suggests that co-ordinated multicellular behaviour, although more subtle than the social behaviour exhibited in myxobacteria, may be more widespread in the proteobacteria than previously thought. By quantifying the spatial dimensions of the seeding microcolonies, we determined that there was a threshold diameter required for phenotypic differentiation of the microcolony (approx. 80 μm in our system), demonstrating a spatio-temporal development. Moreover, while void areas within the hollow mounds gradually increased with cluster expansion, the thickness of the outer wall remained similar, suggesting that the transfer process of exogenous solutes such as nutrients, O_2, etc., into diffusion-limited regions, namely the interior of the biofilm microcolonies, may be important in regulating this phenomenon. Since concentration gradients within the microcolonies will be influenced by the hydrodynamic conditions, nutrient availability and the level of resident microbial activity, the threshold size of the microcolonies required for initiating seeding dispersal may be expected to vary with environmental growth or culture conditions. However, we point out that under the specified growth conditions described, the developmental process of differentiated structures was reproducible and as such served as a suitable method for further analysis of PAO1 isogenic mutants.

Role of rhamnolipid surfactant production in seeding dispersal

PAO1-Δ*rhlA* biofilms also formed hollow structural mounds similar to those in the PAO1 biofilm and were able to detach via the seeding dispersal process (Fig. 2b). The structural dimensions of these hollowed clusters, including the wall thickness, were statistically comparable to those measured in PAO1 biofilms ($P>0{\cdot}7$; data not shown). Although both PAO1 and PAO1-Δ*rhlA* biofilms covered the entire surface of the glass flow cells, the PAO1-Δ*rhlA* strain resulted in a significantly thicker biofilm by the end of the experimental run, consistent with the findings of Davey *et al.* (2003). While the hollow differentiated mounds persisted in PAO1, the hollow colonies of the PAO1-Δ*rhlA* biofilm differentiated earlier in biofilm growth and by day 4 formed a flat homogeneous biomass. This observation can be explained by the findings of Davey *et al.* (2003) where rhamnolipid was important in maintaining the non-colonized channels surrounding biofilm macrocolonies. The transient nature of differentiation and dispersal in PAO1-Δ*rhlA* illustrates the importance of frequent monitoring.

Role of global cell signalling in seeding dispersal

In comparison to PAO1 biofilms, the efficiency with which PAO1-Δ*lasI*Δ*rhlI* was able to colonize the surface area was retarded by up to 2 days. However, unlike Davies *et al.* (1998), the PAO1-Δ*lasI*Δ*rhlI* biofilms were able to differentiate into mature microcolonies in our flow cell system as early as day 2 of the experimental run. This observation was consistent with our previous findings where we demonstrated that homoserine lactone was not required for biofilm formation in which we also utilized LB as a growth substrate (Purevdorj *et al.*, 2002). A total of 97 individual biofilm microcolonies with diameters statistically comparable to PAO1 ($P>0{\cdot}05$; except on day 4 where the PAO1-Δ*lasI*Δ*rhlI* clusters were larger than those in PAO1, $P<0{\cdot}05$) were observed in our flow system, none of which developed hollow mounds. The inability of the PAO1-Δ*lasI*Δ*rhlI* biofilm to seed cannot be attributed to the lack of motility since the three types of motility were not abolished in PAO1-Δ*lasI*Δ*rhlI* on LB agar (data not shown). This suggests involvement of QS in the differentiation process, possibly by sensing cell density and nutrient depletion within the periphery of the biofilm clusters.

Clinical significance of seeding dispersal

It is well known that chronically infected CF patients frequently harbour mucoid variants of *P. aeruginosa* (Høiby *et al.*, 2001). We wished to investigate the clinical relevance of this dispersal phenomenon by analysing biofilms grown from the CF isolate, mucoid *P. aeruginosa* FRD1. Interestingly in all three replicate flow cell experiments, FRD1 biofilms did not form hollow structures, despite the fact that the mean cluster size, as well as general biomass accumulation, did not significantly differ between the two biofilms (all values $P>0{\cdot}05$). Initially we speculated that the inability of FRD1 to undergo differentiation and dispersal could be due to its 'high' viscosity. In general FRD1 biofilms are commonly perceived to be a more viscous counterpart of the wild-type strain due to its voluminous slimy nature. However, the rheometry results showed that FRD1 biofilms were less viscous than those of the environmental non-mucoid strain PAO1 ($P=0{\cdot}014$), which ruled out this hypothesis. Whether the inability of FRD1 to undergo differentiation and 'seed' is due to abolished motility and/or genetic regulation needs to be addressed in future studies. Regardless, the active seeding dispersal process we describe here may not be the method utilized in mucoid variants of

clinical CF isolates, but rather a transmission mechanism utilized by environmental strains of *P. aeruginosa*.

ACKNOWLEDGEMENTS

This work was funded by the National Institutes of Health RO1 grant GM60052 (P. S.) and in part by the W. M. Keck Foundation (P. Stewart). From Montana State University we thank Todd Shaw and Cory Rupp for rheometry, Dr Phil Stewart, Dr Matt Parsek and Dr Michael Franklin for experimental discussions and the latter for providing pMF230. Suzanne Wilson is thanked for experimental assistance. We also thank Dr Morten Hentzer for providing the PAO-Δ*fliM* mutant, Dr Jim Pearson for JP2 and Dr O'Toole for providing PAO1-Δ*rhlA* strains. This paper is to be used as partial fulfilment of the PhD Microbiology degree of B. P.-G.

REFERENCES

Aendekerk, S., Ghysels, B., Cornelis, P. & Baysse, C. (2002). Characterization of a new efflux pump, MexGHI-OpmD, from *Pseudomonas aeruginosa* that confers resistance to vanadium. *Microbiology* **148**, 2371–2381.

Bryers, J. D. (1988). Modeling biofilm accumulation. In *Physiological Models in Microbiology*, vol. 2, pp. 109–144. Edited by M. J. Bazin & J. I. Prosser. Boca Raton, FL: CRC Press.

Characklis, W. G. (1990). Biofilm processes. In *Biofilms*, pp. 195–231. Edited by W. G. Characklis & K. C. Marshall. New York: Wiley.

Davey, M. E., Caiazza, N. C. & O'Toole, G. A. (2003). Rhamnolipid surfactant production affects biofilm architecture in *Pseudomonas aeruginosa* PAO1. *J Bacteriol* **185**, 1027–1036.

Davies, D. G., Parsek, M. R., Pearson, J. P., Iglewski, B. H., Costerton, J. W. & Greenberg, E. P. (1998). The involvement of cell-to-cell signals in the development of a bacterial biofilm. *Science* **280**, 295–298.

Høiby, N., Krogh Johansen, H., Moser, C., Song, Z., Ciofu, O. & Kharazmi, A. (2001). *Pseudomonas aeruginosa* and the *in vitro* and *in vivo* biofilm mode of growth. *Microbes Infect* **3**, 23–35.

Kaplan, J. B., Ragunath, C., Ramasubbu, N. & Fine, D. H. (2003a). Detachment of *Actinobacillus actinomycetemcomitans* biofilm cells by an endogenous β-hexosaminidase activity. *J Bacteriol* **185**, 4693–4698.

Kaplan, J. B., Meyenhofer, M. F. & Fine, D. H. (2003b). Biofilm growth and detachment of *Actinobacillus actinomycetemcomitans*. *J Bacteriol* **185**, 1399–1404.

Klausen, M., Aaes-Jorgensen, A., Molin, S. & Tolker-Nielsen, T. (2003). Involvement of bacterial migration in the development of complex multicellular structures in *Pseudomonas aeruginosa* biofilms. *Mol Microbiol* **50**, 61–68.

Kohler, T., Curty, L. K., Barja, F., van Delden, C. & Pechere, J. C. (2000). Swarming of *Pseudomonas aeruginosa* is dependent on cell-to-cell signaling and requires flagella and pili. *J Bacteriol* **182**, 5990–5996.

Nivens, D. E., Ohman, D. E., Williams, J. & Franklin, M. J. (2001). Role of alginate and its O acetylation in formation of *Pseudomonas aeruginosa* microcolonies and biofilms. *J Bacteriol* **183**, 1047–1057.

Ochsner, U. A., Fiechter, A. & Reiser, J. (1994). Isolation, characterization, and expression in *Escherichia coli* of the *Pseudomonas aeruginosa rhlAB* genes encoding a rhamnosyltransferase involved in rhamnolipid biosurfactant synthesis. *J Biol Chem* **269**, 19787–19795.

Ohman, D. E. & Chakrabarty, A. M. (1981). Genetic mapping of chromosomal determinants for the production of the exopolysaccharide alginate in a *Pseudomonas aeruginosa* cystic fibrosis isolate. *Infect Immun* **33**, 142–148.

Pearson, J. P., Pesci, E. C. & Iglewski, B. H. (1997). Roles of *Pseudomonas aeruginosa las* and *rhl* quorum-sensing systems in control of elastase and rhamnolipid biosynthesis genes. *J Bacteriol* **179**, 5756–5767.

Picioreanu, C., van Loosdrecht, M. C. & Heijnen, J. J. (2001). Two-dimensional model of biofilm detachment caused by internal stress from liquid flow. *Biotechnol Bioeng* **72**, 205–218.

Purevdorj, B., Costerton, J. W. & Stoodley, P. (2002). Influence of hydrodynamics and cell signaling on the structure and behavior of *Pseudomonas aeruginosa* biofilms. *Appl Environ Microbiol* **68**, 4457–4464.

Purevdorj-Gage, B. & Stoodley, P. (2004). Hydrodynamic considerations of biofilm structure and behavior. In *Microbial Biofilms*, pp. 160–173. Edited by M. A. Ghannoum & G. O'Toole. Washington, DC: American Society for Microbiology.

Rashid, M. H. & Kornberg, A. (2000). Inorganic polyphosphate is needed for swimming, swarming, and twitching motilities of *Pseudomonas aeruginosa*. *Proc Natl Acad Sci U S A* **97**, 4885–4890.

Sauer, K., Camper, A. K., Ehrlich, G. D., Costerton, J. W. & Davies, D. G. (2002). *Pseudomonas aeruginosa* displays multiple phenotypes during development as a biofilm. *J Bacteriol* **184**, 1140–1154.

Semmler, A. B., Whitchurch, C. B. & Mattick, J. S. (1999). A re-examination of twitching motility in *Pseudomonas aeruginosa*. *Microbiology* **145**, 2863–2873.

Stewart, P. S. (1993). A model of biofilm detachment. *Biotechnol Bioeng* **41**, 111–117.

Stewart, P. S., McFeters, G. A. & Huang, C. T. (2000). Biofilm formation and persistence. In *Biofilms II: Process Analysis and Application*, pp. 373–405. Edited by J. D. Bryers. New York: Wiley-Liss.

Stoodley, P., Lewandowski, Z., Boyle, J. D. & Lappin-Scott, H. M. (1999). Structural deformation of bacterial biofilms caused by short-term fluctuations in fluid-shear: an in situ investigation of biofilm rheology. *Biotechnol Bioeng* **65**, 83–93.

Stoodley, P., Wilson, S., Hall-Stoodley, L., Boyle, J. D., Lappin-Scott, H. M. & Costerton, J. W. (2001). Growth and detachment of cell clusters from mature mixed-species biofilms. *Appl Environ Microbiol* **67**, 5608–5613.

Stoodley, P., Sauer, K., Davies, D. G. & Costerton, J. W. (2002). Biofilms as complex differentiated communities. *Annu Rev Microbiol* **56**, 187–209.

Tolker-Nielsen, T., Brinch, U. C., Ragas, P. C., Andersen, J. B., Jacobsen, C. S. & Molin, S. (2000). Development and dynamics of *Pseudomonas* sp. biofilms. *J Bacteriol* **182**, 6482–6489.

Towler, B. W., Rupp, C. J., Cunningham, A. B. & Stoodley, P. (2003). Viscoelastic properties of a mixed culture biofilm from rheometer creep analysis. *Biofouling* **19**, 279–285.

Van Loosdrecht, M. C. M., Eikelboom, D., Gjaltema, A., Mulder, A., Tijhuis, L. & Heijnen, J. J. (1995). Biofilm structures. *Water Sci Technol* **32**, 35–43.

Van Loosdrecht, M. C. M., Picioreanu, C. & Heijnen, J. J. (1997). A more unifying hypothesis for the structure of microbial biofilms. *FEMS Microb Ecol* **24**, 181–183.

Webb, J. S., Thompson, L. S., James, S., Charlton, T., Tolker-Nielsen, T., Koch, B., Givskov, M. & Kjelleberg, S. (2003). Cell death in *Pseudomonas aeruginosa* biofilm development. *J Bacteriol* **185**, 4585–4592.

Wilson, S., Hamilton, M. A., Hamilton, G. C., Schumann, M. R. & Stoodley, P. (2004). Statistical quantification of the detachment rates and size distribution of cell clumps from wild type (PAO1) and cell signaling mutant (JP1) *Pseudomonas aeruginosa* biofilms. *Appl Environ Microbiol* **70**, 5847–5852.